A new arbitrary reference configuration (ARC) formulation for computational finite strain transient applications

Xiangmin Zhou, Kumar K. Tamma*, Desong Sha

Army High Performance Computing Research Center (AHPCRC) University of Minnesota, Minneapolis, MN 55455, USA

Abstract

A new arbitrary reference configuration (ARC) elasticity theory is proposed in the paper for finite strain dynamic applications with both the attempt to circumvent the deficiencies associated with the hyperelasticity and hypoelasticity theories. The corresponding stress update formulation and the ARC Lagrangian formulation is also developed. Some numerical examples are shown to demonstrate the effectiveness of the proposed theory.

Keywords: Finite strain; Large deformation; Elasticity theory; Elasto-plasticity; Stress update formulation

1. Introduction

In computational finite strain dynamic analysis of isotropic elasto-plastic materials three major aspects are involved: the constitutive models, the finite element formulations, and the time integration methods. This paper focuses on the constitutive models and the finite element formulations. Besides the plasticity of the material, two kinds of the elasticity models are primarily used for the computational finite strain dynamic analysis: the Saint-Venant-Kirchhoff grade one hyperelasticity and the Jaumann stress rate grade zero hypoelasticity. In terms of the finite element formulations with Lagrangian mesh, the total Lagrangian (TL) formulation and the updated Lagrangian (UL) formulation are widely used. However, for finite deformation analysis there are some drawbacks associated with the existing approaches: (i) the Saint-Venant-Kirchhoff grade one hyperelasticity is not suitable to model finite strain phenomena [1]; (ii) the multiplicative decomposition approach for Saint-Venant-Kirchhoff hyperelasto-plasticity will result in non-symmetric plastic flow rule [2]; (iii) the incremental stiffness matrix for the Jaumann stress rate grade zero hypoelasticity is nonsymmetric [3]; (iv) the update Lagrangian formulation requires iterations to achieve the current configuration [4]. With the attempt to overcome the aforementioned drawbacks, we propose here a new arbitrary reference configuration (ARC) elasticity theory and the corresponding arbitrary reference configuration Lagrangian formulation.

* Corresponding author. Tel.: +1 612 626 8102; Fax: +1 612 626 1596; E-mail: ktamma@tc.umn.edu

Computational Fluid and Solid Mechanics 2005
K.J. Bathe (Editor)

2. Constitutive models

We first consider two simple constitutive models: (i) the Saint-Venant-Kirchhoff model (grade one hyperelasticity), and (ii) the grade zero Truesdell stress rate hypoelasticity model. Then we propose the ARC elasticity theory.

2.1. Hyperelasticity

Here we consider the simplest of the hyperelastic models, namely, the Saint-Venant-Kirchhoff model, of which the stored energy function is given by $\varphi(\mathbf{E}^t_{t_0}) = \frac{\lambda}{2}(tr\mathbf{E}^t_{t_0}) + \mu tr(\mathbf{E}^t_{t_0})^2$, where $\mathbf{E}^t_{t_0}$ is the Saint-Venant-Green strain tensor. The stress–strain relation is given by $\mathbf{S}^t_{t_0} = \mathcal{C} : \mathbf{E}^t_{t_0}$, where $\mathcal{C} = \lambda\mathbf{I}\otimes\mathbf{I} + 2\mu\mathcal{I}$ is the elasticity tensor and $\mathbf{I}$ is the second-order identity tensor, $\mathcal{I}$ is the fourth-order identity tensor, λ and μ are the Lamé material coefficients, and $\mathbf{S}^t_{t_0}$ is the second Piola–Kirchhoff stress tensor.

Let $t_\gamma = (1-\gamma)t_\alpha + \gamma t$, $\forall_\gamma \in \Re$, and $t_{mid} = t_{\gamma=\frac{1}{2}}$ and further considering the relations, $\sigma^{t_\alpha}_{t_\gamma} = J^{t_\alpha}_{t_\gamma}\mathbf{F}^{t_\gamma}_{t_\alpha}\sigma_{t_\alpha}(\mathbf{F}^{t_\gamma}_{t_\alpha})^T$, $(\epsilon_{t_\gamma})^t_{t_\alpha} = (\mathbf{F}^{t_\alpha}_{t_\gamma})^T\mathbf{E}^t_{t_a}\mathbf{F}^{t_\alpha}_{t_\gamma}\mathbf{F}^t_{t_a} = \mathbf{F}^t_{t_\gamma}\mathbf{F}^{t_\alpha}_{t_\gamma}$, and $J^{t_\gamma}_t = J^{t_\alpha}_t J^{t_\gamma}_{t_\alpha}$, the constitutive equation then can be mapped into the t_γ configuration as

$$\sigma_t = J_t^{t_\gamma}\mathbf{F}_{t_\gamma}^t\left[\sigma_{t_\gamma}^{t_\alpha} + C_{t_\gamma}^{t_0} : (\epsilon_{t_\gamma})_{t_\alpha}^t\right](\mathbf{F}_{t_\gamma}^t)^T \tag{1}$$

2.2. Hypoelasticity

Hypoelasticity is mostly defined through corotational stress rates such as the Zaremba–Jaumann–Noll rate, the Green–McInnis–Naghdi rate, the twirl tensor of Eulerian triad stress rate, and the logarithmic stress rate. Due to the fact that the corotational stress rates relate to the Lagrangian stress or the Lagrangian stress rate through the Truesdell stress rate, the resulting mapped Lagrangian elasticity modulus only possesses minor symmetry but does not possess major symmetry when the grade zero corotational stress rate hypoelasticity is employed. To obtain the major symmetry of the elasticity modulus for grade zero hypoelasticity, the use of the Truesdell rate grade zero hypoelasticity has been suggested in the literature. Here we adapt the Truesdell rate grade zero hypoelasticity, which is given as $\mathring{\sigma}^{\tau} = \mathcal{C} : \mathcal{D}$, and subject to the initial conditions $\sigma(t_\alpha) = \sigma_{t\alpha}$, where the elasticity tensor $\mathcal{C}$ is constant, and the velocity strain $\mathcal{D}$ and the Truesdell rate of Cauchy stress $\mathring{\sigma}^{\tau}$ are one-point tensors. Therefore, the hypoelasticity model is path dependent, and numerical integration along the deformation path to obtain the Cauchy stress at time t is necessary. In order to perform the numerical integration over a certain time period, the Truesdell rate grade zero hypoelasticity of equation needs to be mapped to a fixed configuration. Considering the relations: $\sigma_{t_{mid}}^{t_\alpha} = J_{t_{mid}}^{t_\alpha}\mathbf{F}_{t_\alpha}^{t_{mid}}\sigma_{t_\alpha}(\mathbf{F}_{t_\alpha}^{t_{mid}})^T$, $(\epsilon_{t_{mid}})_{t_\alpha}^t = (\mathbf{F}_{t_{mid}}^{t_\alpha})^T\mathbf{F}_{t_\alpha}^t$, $\mathbf{F}_{t_{mid}}^t = \mathbf{F}_{t_\alpha}^t\mathbf{F}_{t_{mid}}^{t_\alpha}$ and $J_t^{t_{mid}} = J_t^{t_\alpha}J_{t\alpha}^{t_{mid}}$, the Cauchy stress becomes:

$$\mathcal{Z}_{t_{mid}}^t = \sigma_{t_{mid}}^{t_\alpha} + \mathcal{C} : (\epsilon_{t_{mid}})_{t_\alpha}^t \tag{2}$$

Thus we have a second-order accurate stress update formulation for the grade zero Truesdell stress rate hypoelasticity.

2.3. ARC elasticity

Replacing the Green strain measure by the ARC Green strain measure in the hyperelasticity models yields a new class of elasticity models which we term as the ARC elasticity. For example, the Saint-Venant-Kirchhoff hyperelasticity can be modified to yield the simplest model for ARC elasticity, of which the stored energy function is given by $\varphi_{t_0}^t = \sum_{i=1}^{\alpha}\varphi_{t_{i-1}}^{t_i} + \varphi_{t_a}^t$ and $\varphi_{t_\alpha}^t = \frac{\lambda}{2}(tr\mathbf{E}_{t_\alpha}^t)^2 + \mu tr(E_{t_\alpha}^t)^2$. The ARC stress–strain relation thus is given by $\mathbf{Z}_{t_\alpha}^t = \mathcal{C} : \mathbf{E}_{t_\alpha}^t$, where $\mathcal{C} = \lambda\mathbf{I}\otimes\mathbf{I} + 2\mu\mathcal{I}$.

Following the derivation described previously, the Cauchy stress is obtained as:

$$\mathcal{Z}_{t_a}^t = \sigma_t + \mathcal{C} : \mathbf{E}_{t_\alpha}^t \tag{3}$$

Thus the ARC elasticity can recover Eq. (1) by setting $\mathcal{C}_{t_\alpha}^{t_0} = \mathcal{C}$.

2.4. Rate constitutive equations of plasticity

For non-softening plasticity, the principle of maximum plastic dissipation (or the maximum dissipation postulate) [5], is described by $(\varsigma - \sigma, \mathcal{D} - (\mathcal{C}^*)^{-1} : \mathring{\sigma}^{\tau}) \le 0$, $\sigma \in \Re^3\times\Re^3$, $\mathcal{F}(\sigma) \le 0$ $\mathcal{F}(\varsigma) \le 0$, $\forall\varsigma \in \Re^3\times\Re^3$, where $\mathcal{F}$: $\Re^3\times\Re^3 \mapsto \Re$ is a convex yield function in the Cauchy stress space and $\mathcal{C}^*$ is the elastic modulus. The principle of maximum plastic dissipation implies an associative (normality) flow rule in Cauchy stress space for plasticity strain rate. Introducing a Lagrangian multiplier $\lambda^p \in \Re$ into the variational inequality of equation, yields the stress–strain relation and the Kuhn–Tucker complementarity form of loading/unloading conditions for non-softening plasticity can also be derived from the Drucker's hardening postulate. Thus:

$$\mathring{\sigma}^{\tau} = \mathcal{C}^* : [\mathcal{D} - \lambda^p\nabla_\sigma\mathcal{F}(\sigma)] \tag{4}$$

$$\mathcal{F}(\sigma) \le 0, \quad \lambda \ge 0, \quad \lambda^p\mathcal{F}(\sigma) = 0 \tag{5}$$

3. Stress update formulation

From the discussion in the previous section we have the following stress update formulation for elasticity as:

$$\sigma_t = J_t^{t_\gamma}\mathbf{F}_{t_\gamma}^t\left[\sigma_{t_\gamma}^{t_a} + \mathcal{C}^* : (\epsilon_{t_\gamma})_{t_\alpha}^t\right](\mathbf{F}_{t_\gamma}^t)^T \tag{6}$$

For hyperelasticity, choose

$$\mathcal{C}^* = \mathcal{C}_{t_g}^{t_0} = \mathbf{J}_{t_\gamma}^{t_{\bar\gamma}}\left[{}^{iI}\mathbf{F}_{t_\gamma}^{t_{\bar\gamma}}\right]\left[{}^{jJ}\mathbf{F}_{t_\gamma}^{t_{\bar\gamma}}\right]\left[{}^{kK}\mathbf{F}_{t_\gamma}^{t_{\bar\gamma}}\right]\left[{}^{lL}\mathbf{F}_{t_\gamma}^{t_{\bar\gamma}}\right]\left[{}^{IJKL}\mathbf{F}_{t_{\bar\gamma}}^{t_0}\right],$$

where $t_{\bar\gamma} = t_\gamma - \Delta t$ and $\mathcal{C}_{t_0}^{t_0} = \mathcal{C}$. For hypoelasticity, choose $t_\gamma = t_{mid}$ and $\mathcal{C}^* = \mathcal{C}$. For the ARC elasticity, choose $t_\gamma = t_\alpha$ and $\mathcal{C}^* = \mathcal{C}$.

3.1 Weak form of constitutive equation

Let $\mathcal{D}(\mathbf{w})$ be the variation of the velocity strain $\mathcal{D}(\mathbf{v})$. According to the definition of the variation, the variation of the ARC Green strain tensor $\delta\mathbf{E}_{t_\alpha}^t(\mathbf{w})$ is obtained as $\delta\mathbf{E}_{t_\alpha}^t(\mathbf{w}) = (\mathbf{F}_{t_\alpha}^t)^T\mathcal{D}(\mathbf{w})\mathbf{F}_{t_\alpha}^t$. Similarly, we have the relationship of the variations between $D(\mathbf{w})$ and $\delta(\epsilon_{t_\gamma})_{t_\alpha}^t(\mathbf{w})$ as $\delta(\epsilon_{t_\gamma})_{t_\alpha}^t(\mathbf{w}) = (\mathbf{F}_{t_\gamma}^t)^T\mathcal{D}(\mathbf{w})\mathbf{F}_{t_\gamma}^t$.

Let Ω_{t_γ} be the domain of the body at a reference configuration at time t_γ, and again considering the relationship of the variation between $\mathcal{D}(\mathbf{w})$ and $\delta(\epsilon_{t_\gamma})_{t_\alpha}^t(\mathbf{w})$, the weak form of the constitutive equation becomes:

$$(\mathcal{D}(\mathbf{w}), \sigma(t))_{\Omega_t} = (\delta(\epsilon_{t_\gamma})_{t_\alpha}^t(\mathbf{w}), \sigma_{t_\gamma}^{t_\alpha} + \mathcal{C}^* : (\epsilon_{t_\gamma})_{t_\alpha}^t)_{\Omega_{t_\gamma}} \tag{7}$$

Remark 1

1. Equation (7) is termed as the ARC Lagrangian formulation.
2. When setting $t_\gamma = t_0$, equation (7) corresponds to the total Lagrangian formulation.
3. When setting $t_\gamma = t$, equation (7) corresponds to the updated Lagrangian formulation.

The illustrations of the ARC Lagrangian formulation, the total Lagrangian formulation, and the updated Lagrangian formulation are shown in Figs. 1(a)–1(c), respectively.

4. Numerical examples

The numerical simulation of the Taylor impact test [6] is performed to verify the present developments. The Taylor impact test fires a solid cylinder against a massive rigid target with a flat surface, and then measures the deformed length and the diameter of the solid cylinder. The Taylor impact test uses high-strength low-alloy HSLA 100 high strength steel with impact velocity of 245.7 m/s^{-1} as shown in [6]. The configuration of the HSLA 100 high-strength steel cylinder is given by the initial length L_0 of 38 mm and initial radius R_0 of 3.795 mm. The material parameters of the Zerilli–Armstrong strength model fitted by the split Hopkinson pressure bar (SHPB) test data for the (HSLA) 100 high-strength steel are obtained from [6]. The simulation is performed by modeling one quarter of the cylinder with a total 19 712 nodes and 17 163 8-noded brick elements. The time integration method of the algorithm employs the forward displacement central difference (FDCD) method. The simulation was performed using 8000 time steps and the final time is 70 μs with the time step of 0.875×10^{-8} s. The final configuration and the von Mises effective plastic strain distribution at a time of 70 μs of the simulation for both the ARC model and Jaumann rate model are shown in Fig. 2(b) and 2(c). The simulation results in comparison with the experimental result are shown in Table 1. The average error $\bar{\Delta}$ is computed by, $\bar{\Delta} = \frac{1}{2}\left(\frac{|\Delta L|}{L*} + \frac{|\Delta R|}{R*}\right)$, where ΔL and ΔR are the difference of the final length and radius for the simulation with respect to the experimental values, and $L*$ and $R*$ are the final length and radius of experimental values. The simulation results for the ARC model and the Jaumann rate model are almost identical. Both the ARC model result and the Jaumann rate model result agree well with the experimental result. The ARC model consumed about 20% less CPU time than that of the Jaumann rate model. The additional CPU time consumed by the Jaumann rate model is primarily due to the Polar decomposition of the incremental deformation gradient tensor which is required by the Jaumann rate model.

5. Remarks

There are numerous issues associated with the current approaches for computational finite strain dynamic analysis of isotropic elasto-plasticity materials. With the attempt to resolve these issues, we proposed to employ the incremental infinitesimal strain measure to compute the incremental stress and then map exactly the total stress to the current configuration as the arbitrary reference configuration, namely, the ARC Lagrangian formulation and the corresponding ARC elasticity. The stress update formulations for the ARC Lagrangian formulation were then derived. Finally, numerical simulations were shown to demonstrate the effectiveness of the ARC Lagrangian formulation for finite deformation problems in comparison with the total Lagrangian (or the equivalent updated Lagrangian formulation).

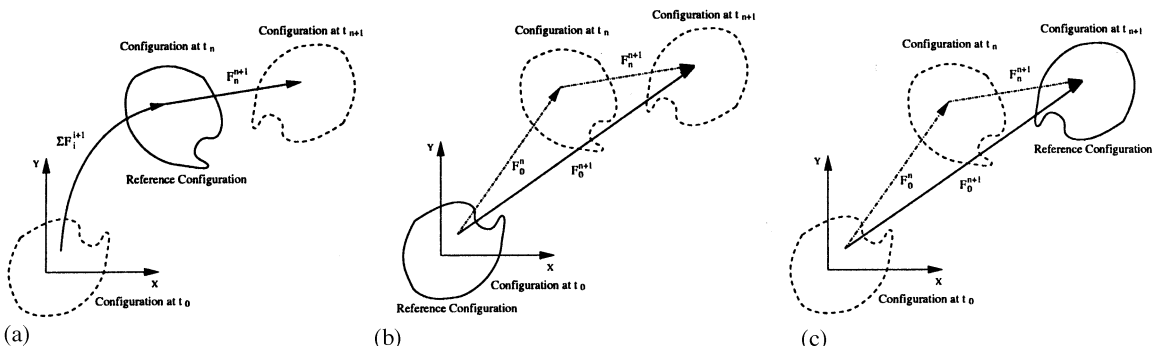

Fig. 1. Illustration of ARC Lagrangian formulation (a), total Lagrangian formulation (b), and updated Lagrangian formulation (c).

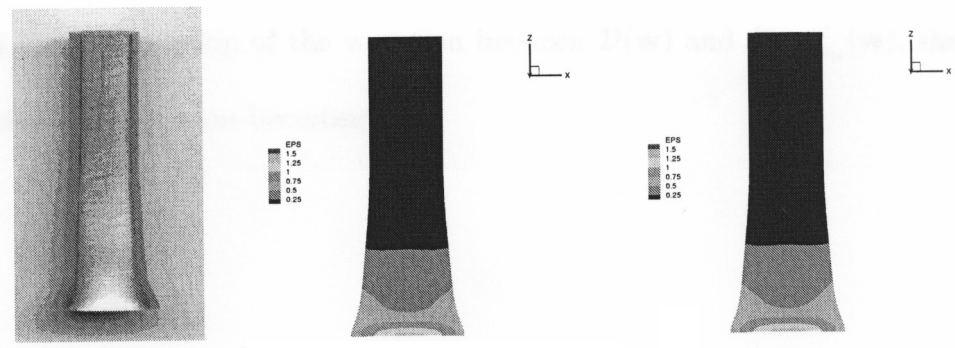

(a) (b) (c)

Fig. 2. Experiment and numerical results of Taylor impact test. (a) Experiment result [6]. (b) ARC model result. (c) Jaumann rate result. (Fig. 2a reproduced with permission from [6].)

Table 1
Comparison of Taylor impact test numerical simulation with experimental results for the HSLA 100 high-strength steel

	Exp. [6]	ARC	Jaumann rate
L^*/L_0	0.838	0.819 (−2.26%)	0.819 (−2.26%)
R^*/R_0	1.581	1.561 (−1.67%)	1.561 (−1.67%)
$\bar{\Delta}$	N/A	1.965%	1.965%
ε_p^{max}	N/A	1.4208	1.4202
CPU (s)	N/A	18,104	21,668

6. Acknowledgments

The authors are very happy to acknowledge support in part by Battelle/US Army Research Office (ARO) Research Triangle Park, North Carolina, under grant number DAAH04-96-C-0086, and by the Army High Performance Computing Research Center (AHPCRC) under the auspices of the Department of the Army, Army Research Laboratory (ARL) under contract number DAAD19–01–2–0014. Dr. Raju Namburu is the technical monitor. The content does not necessarily reflect the position or the policy of the government, and no official endorsement should be inferred. Other related support in the form of computer grants from the Minnesota Supercomputer Institute (MSI), Minneapolis, Minnesota is also gratefully acknowledged.

References

[1] Simo JC, Hughes TJR. Computational Inelasticity. New York: Springer, 1998.
[2] Simo JC. Algorithm for static and dynamic multiplicative plasticity that preserve the classical return mapping schemes of the infinitesimal theory. Comp Meth in App Mech and Eng 1992;99:61–112.
[3] Belytschko T, Liu WK, Moran B. Nonlinear Finite Elements for Continua and Structures. New York: J. Wiley and Sons, 2000.
[4] Bathe KJ. Finite Element Procedures in Engineering Analysis. Englewood Cliffs, NJ: Prentice-Hall, 1996.
[5] Hill R. The Mathematical Theory of Plasticity. Oxford: Oxford University Press, 1950.
[6] Hanson KM, Hemez FM. Bayesian calibration of simulation models using experimental data. In: Proc of NECDC 2002, Monterey, CA, 21–24 October, 2002.